



OPEN ACCESS

EDITED BY
Zhongqi Fan,
Fujian Agriculture and Forestry
University, China

REVIEWED BY
Meilin Li,
Shenyang Agricultural University, China
Tao Luo,
South China Agricultural University,
China

*CORRESPONDENCE
Longqing Chen,
chenlq@swfu.edu.cn

[†]These authors have contributed equally
to this work

SPECIALTY SECTION
This article was submitted to Plant
Genomics,
a section of the journal
Frontiers in Genetics

RECEIVED 01 October 2022
ACCEPTED 31 October 2022
PUBLISHED 22 November 2022

CITATION
Geng F, Nie R, Yang N, Cai L, Hu Y,
Chen S, Cheng X, Wang Z and Chen L
(2022), Integrated transcriptome and
metabolome profiling of *Camellia
reticulata* reveal mechanisms of flower
color differentiation.
Front. Genet. 13:1059717.
doi: 10.3389/fgene.2022.1059717

COPYRIGHT
© 2022 Geng, Nie, Yang, Cai, Hu, Chen,
Cheng, Wang and Chen. This is an
open-access article distributed under
the terms of the [Creative Commons
Attribution License \(CC BY\)](https://creativecommons.org/licenses/by/4.0/). The use,
distribution or reproduction in other
forums is permitted, provided the
original author(s) and the copyright
owner(s) are credited and that the
original publication in this journal is
cited, in accordance with accepted
academic practice. No use, distribution
or reproduction is permitted which does
not comply with these terms.

Integrated transcriptome and metabolome profiling of *Camellia reticulata* reveal mechanisms of flower color differentiation

Fang Geng^{1†}, Ruimin Nie^{1†}, Nan Yang¹, Lei Cai², YunChong Hu¹, Shengtong Chen¹, Xiaomao Cheng¹, Zhonglang Wang² and Longqing Chen^{1*}

¹College of Landscape Architecture and Horticulture Sciences, Southwest Landscape Architecture Engineering Technology Research Center of National Forestry and Grassland Administration, Yunnan Functional Flower Resources and Industrialization Technology Engineering Research Center, Southwest Forestry University, Kunming, Yunnan, China, ²Kunming Institute of Botany, Chinese Academy of Science, Kunming, Yunnan, China

Camellia reticulata (Lindl.) is an important ornamental plant in China. Long-term natural or artificial selections have resulted in diverse phenotypes, especially for flower colors. Modulating flower colors can enhance the visual appeal and economic value in ornamental plants. In this study, we investigated the molecular mechanisms underlying flower color differentiation in *C. reticulata*. We performed a combined transcriptome and metabolome analysis of the petals of a popular variety *C. reticulata* (HHYC) (red), and its two cultivars “Xuejiao” (XJ) (pink) and “Tongzimian” (TZM) (white). Targeted metabolome profiling identified 310 flavonoid compounds of which 18 anthocyanins were differentially accumulated among the three samples with an accumulation pattern of HHYC > XJ > TZM. Likewise, transcriptome analysis showed that carotenoid and anthocyanin biosynthetic structural genes were mostly expressed in order of HHYC > XJ > TZM. Two genes (*gene-LOC114287745765* and *gene-LOC114289234*) encoding for anthocyanidin 3-O-glucosyltransferase are predicted to be responsible for red coloration in HHYC and XJ. We also detected 42 MYB and 29 bHLH transcription factors as key regulators of anthocyanin-structural genes. Overall, this work showed that flavonoids, particularly anthocyanins contents are the major determinants of flower color differentiation among the 3 *C. reticulata* samples. In addition, the main regulatory and structural genes modulating anthocyanin contents in *C. reticulata* have been unveiled. Our results will help in the development of *Camellia* varieties with specific flower color and quality.

KEYWORDS

omics, anthocyanins, carotenoids, flower, *Camellia reticulata*

1 Introduction

Camellia reticulata (Lindl.), also known as Yunnan camellia is among the decorative trees belonging to the *Camellia* genus, which are members of the Theaceae family (Xia, 2003; Xin et al., 2015). There are 97 different species of *Camellia*, 76 of which are endemic to China (Yu, 1985; Xia, 2003; Zhang et al., 2019). China is considered the origin and distribution hub of *Camellia*. Generally, members of the genus *Camellia* are classified into one of five groups. Yunnan camellia (*C. reticulata*) and its near relatives constitute a significant group that is primarily found in Yunnan Province. In Yunnan province, *Camellia* is regarded as an exceptional ornamental plant with high economic values. Some of them are very important flowering ornamentals that also produce oil, and have a wide variety of cultivars (Silan et al., 2013; Xin et al., 2015). In addition to its cultural and medicinal significance, *C. reticulata* is also a valuable source of food products (Xia, 2003; Silan et al., 2013; Xin et al., 2015). *C. reticulata* is mostly red-colored, and there are few accounts of color variations in the species. As a result, producers and researchers have constantly sought to breed *C. reticulata* of diverse colors to enhance its aesthetic value (Xin et al., 2015).

Flower color is a key feature of horticultural crops, directly linked to pigments' content and distribution (Zhao and Tao, 2015). Numerous studies have revealed that carotenoids, flavonoids, and alkaloids are among the most important pigments that contribute to the development of flower colors (Wang et al., 2001; Ma et al., 2018; Zhu et al., 2019). Particularly, carotenoids and flavonoids have garnered increasing interest as they are pigments extensively dispersed in plants and are responsible for the spectacular hues found in petals (Mekapogu et al., 2020; Cui et al., 2021; Gao et al., 2021; Mei et al., 2021). Carotenoids can cause flowers to display a wide spectrum of colors, from vivid red to orange to yellow (Clotault et al., 2008; Tanaka et al., 2008; Zhao and Tao, 2015). Likewise, flavonoids, which are the most significant secondary metabolites in plants, can create colors ranging from light yellow to purple, depending on the type of flavonoids. *Camellia* blooms have been the subject of recent studies due to the plant's status as an ornamental plant. Carotenoids and flavonol glycosides were revealed to be the primary pigments in the golden yellow blooms of the *C. nitidissima* by Zhou et al. (2017). The pigment composition of red-flowered *Camellia* species was investigated by Jianbin Li et al. (2013), who concluded that cyanidin-core structure pigments (such as cyanidin 3,5-di-O-glucoside) have the potential to produce the most dominant phenotype among wild red-flowered *Camellia* species in China. According to Norihiko et al. (2001), the red blossoms of *Benibana-cha* also contain anthocyanins, albeit in somewhat different proportions. In spite of findings from a recent study that anthocyanins are not present in many white and yellow flowers of ornamental plants (Chen et al., 2012), practically all of the core metabolites needed for anthocyanin

production are found in the white grape hyacinth petal (Lou et al., 2014). In a similar vein, the sepals of developing white tea flowers (*C. sinensis*) contain maximum levels of proanthocyanidins between the stages of complete separation and full bloom (Joshi and Gulati, 2011; Yu et al., 2020).

Anthocyanins are one of the most significant secondary metabolites that plants produce, and research has shown that they possess anti-cancer, anti-oxidation, and anti-atherosclerosis characteristics (Escribano-Bailon and Santos-Buelga, 2012; Jiang et al., 2021). Anthocyanins are responsible for the orange, red, magenta, violet, and blue flower colorations. The biochemical route that leads to petal pigment accumulation has been thoroughly studied, and the genes that code for the necessary enzymes and transcriptional factors have been identified (Escribano-Bailon and Santos-Buelga, 2012; Feng et al., 2013). Extensive research on the molecular mechanisms involved in the anthocyanin biosynthesis pathway (ABP) has been conducted. However, the majority of previous studies focused mostly on the coloration of fruits and leaves, while anthocyanin production in colored-petals is yet to be studied in *C. reticulata*. Anthocyanin biosynthesis and accumulation is a highly complicated process that is controlled by a number of enzymes, transcription factors, and influenced by varied external environmental factors such as light, water stress, and temperature (He and Giusti, 2010; Hu et al., 2015; Gao et al., 2021). As a result, additional research is required to get complete insights into the mechanism that underlies petal coloration in *C. reticulata*.

Early biosynthetic genes (EBGs) and late biosynthetic genes (LBGs) are the two categories of ABP genes that are found in dicots, along with *phenylalanine ammonia-lyase* (*PAL*) genes (Medda et al., 2021). The genes, *chalcone synthase* (*CHS*), *chalcone isomerase* (*CHI*), and *flavanone 3-hydroxylase* (*F3H*) that are part of the common flavonoid biosynthesis pathway are included in the EBGs. These genes have an effect on downstream flavonoids; while LBGs consist of *F3'H*, *flavonoid 3', 5' hydroxylase* (*F3'5'H*), *dihydroflavonol 4-reductase* (*DFR*), and *anthocyanidin synthase* (*ANS*) as well as *UDP-glucose:flavonoid 3-O-glucosyltransferase* (*UGTs*) (Ren et al., 2021). Flowers come in a variety of colors, and these colors are determined by a number of factors, including co-pigments, cell structure, pH, and other factors (Stavenga et al., 2021). There is a correlation between the *MYB-bHLH-WD40* (MBW) complex and the transcriptional regulation of ABP. MYB (Allan et al., 2008; Fraser et al., 2013; Naik et al., 2021) and bHLH (Li et al., 2020a) are two of the components of this complex that act as positive regulators of ABP genes. In most cases, the expressions of these two components are unique to pigmented tissues. On the other hand, WD40 is found to perform analogous functions in pigmented and non-pigmented tissues alike. Despite this, WD40 is able to maintain the stability of the MBW complex (Hichri et al., 2011; Li et al., 2020b).

Transcriptome and metabolome high-throughput sequencing technology have been widely used in recent years to explore diverse plants' color mechanisms. We performed transcriptome and metabolome profiling, annotation, and bioinformatics analysis to understand the molecular mechanism of *C. reticulata* petal color formation and differentiation. The results of this study will aid in the breeding of cultivars with specific-flower colors.

2 Materials and methods

2.1 Plant materials

Materials tested were *C. reticulata* flowers harvested from three different genotypes that had distinct blossom colors: A popular *C. reticulata* stock (red flower, 'HHYC') and its two cultivars *C. reticulata* 'Xuejiao' (pink flower, XJ), and *C. reticulata* 'Tongzimian' (white flower, TZM). Plant materials were collected in Zixi Mountain of Chuxiong (H: 2133m, E: 101°24'1", N: 25°0'7"), Yunnan, China. They were planted at the experimental station of the College of Landscape and Horticulture, Southwest Forestry University (H:1950m, E: 102°45'53", N:25°4'0"), Kunming, Yunnan, China. Flowers were sampled during blooming in March 2021. There was a total of 9 *C. reticulata* flowers (petals) used in this experiment. As a result, all of the data were acquired based on the three distinct biological replicates that were gathered for each sample. All of the fresh *C. reticulata* petals were flash frozen in liquid nitrogen, and then placed in an ice chest and stored in -80°C refrigerator until further use.

2.2 RNA sequencing

The methods for isolating RNA, purifying, and monitoring it, as well as building a cDNA library and sequencing, were adapted from Sterling et al. (2015). The Qubit® RNA Assay Kit in Qubit® 2.0 Fluorometer (Life Technologies, Carlsbad, CA, United States), the RNA Nano 6000 Assay Kit of the Agilent Bioanalyzer 2100 system (Agilent Technologies, Santa Clara, CA, United States), and the NanoPhotometer® spectrophotometer (IMPLEN, Westlake Village, CA, United States) were used to check, measure, and evaluate the purity, concentration, and integrity. The sequencing libraries were prepared with the NEBNext® Ultra™ RNA Library Prep Kit for Illumina® (NEB, Ipswich, MA, United States) in accordance with the recommendations by the manufacturer, and they were sequenced using an Illumina HiSeq platform. The NEBNext® Ultra™ RNA Library Prep Kit for Illumina® (NEB, Ipswich, MA, United States) was used to prepare sequencing libraries, which were then sequenced using an Illumina HiSeq platform. This was done in accordance with the instructions provided by the manufacturer.

2.3 Identification of differentially expressed genes and transcription factors

With the help of the iTAK software (Zheng et al., 2016), transcription factors were identified. Previous methods by Zhao et al. (2012); Fraser et al. (2013) and Li et al. (2018) were adapted for both the identification and classification of transcription factors. Using a model of negative binomial distribution as a foundation, the DESeq R package (1.10.1) (Anders, 2010) was utilized to perform differential expression analysis. The false discovery rate was purposefully kept under control by the altered *p* values, which were changed using the methodology developed by Benjamini and Hochberg (1995). Genes were considered to have differential expression if their adjusted *p*-value was less than 0.05.

2.4 Real-time quantitative PCR

The RevertAid™ First Strand cDNA synthesis kit was utilized to analyze approximately 1 µg of total RNA in preparation for cDNA synthesis (Thermo Fisher Scientific, Waltham, MA, United States). An amplified reaction was carried out in a volume of L using the LightCycler® 480 real-time PCR equipment in conjunction with a 96-well plate. Each reaction mix contained 1.0 µl of cDNAs, SYBR Premix ExTaq™ 10 µl, PCR forward primer (10 µmol·L⁻¹) 0.5 µl, PCR reverse primer (10 µmol·L⁻¹) 0.5 µl, ddH₂O 8.0 µL, to a final volume of 20 µL. The amplified reaction began with 95°C, maintained for 5 min, and was then followed by 45 cycles of 10 s at 95°C, 20 s at 60°C, and 20 s at 72°C. After each experiment was finished, a melt-curve analysis was performed with the default parameters (5 s at 95°C and 1 min at 65°C). Normalization was accomplished with *β-actin* gene as control (Selvey et al., 2001; Tang et al., 2022). Every analysis was carried out in triplicate with separate biological replicates serving as controls. Table 1 contains a listing of the primer sequences.

2.5 Extraction of metabolites

Metabolites were extracted using a 50% methanol buffer after the samples were thawed on ice (50% solution of methanol in distilled water). Following incubation at room temperature for 10 min and vortexing for 1 min to extract the 20 µl of sample in 120 µl of precooled 50% methanol, the extraction liquid was stored overnight at 60°C. In 96-well plates, the supernatants were transferred following a 20-min centrifugation at 4000 rpm. The extraction and subsequent analysis of data was conducted in three separate instances. An ultra-performance liquid chromatography (UPLC) system was used for all chromatographic separations (SCIEX, Cheshire, United Kingdom). The reversed phase separation was performed using an ACQUITY UPLC BEH Amide

TABLE 1 Primer sequences used for the qRT-PCR validation.

Gene name	Forward primer	Reverse primer
gene-LOC114289234	TCAATCACTTCCATTCTCTCA	CGAGTGCTAACTCCCATTCTT
gene-LOC114285765	CAGTTGATTCGCCAGTGATACA	TTTATCTAGGCATGAGGGTGTCT
gene-LOC114285774	GGTATTTCCATCTCAGGATTGC	TACCTTACCTAGACCTGGCGAA
gene-LOC114288492	TTCCITTTTCATGGTTGTAGAGC	GAACTGGATCGTGTAACCTTCATT
gene-LOC114277682	GTACCCGTCGTATTTGCTTCTC	GATCATATTTGTGCAGTGTCCG
gene-LOC114287489	GTATCCAAATCCATGCAACTCA	TTCCCCATAGCCAAGAATAGAA
gene-LOC114299010	CGTATCTGTGGCTACTGCTGTT	ATCTCCCGCTCCAGGTATTATT
gene-LOC114300537	TTGCCCATAAATACAGAACCTC	AGGAGAAAAGGAGGCATTTACC
gene-LOC114316923	TGGCGAGATATACCCCATCTAT	ACTACGCCTATTGCTTAGACCG
gene-LOC114267429	TCAATCACTTCCATTCTCTCA	CGAGTGCTAACTCCCATTCTT
gene-LOC114322364	CGAGAAGGGCTTATTGACCTA	GAAAGGAAGAACTCAGCTTTT
gene-LOC114280872	TCTATCACTTTGCCCTCTTTT	TTCCGTTGAGAAAAACAACCTACG
gene-LOC114268760	AGCCACTATGAGCCTACTGCAT	GAACCGATGACTTACGCCTTAC
gene-LOC114257730	CAACACCACCAACGCATATC	AGCAACGATTCACGACATTG
gene-LOC114257731	GGGGTGAGTATTTCCGGGAGT	TCCATGCATCTTTTACACTGAA
gene-LOC114257999	GTCCGTCAACTCGATCACCT	TTCAACCAAACCCCATCATT
gene-LOC114258462	GCCATTTCTTCATTGGTGC	GCATTTCAATTTTTCACCCC
gene-LOC114258463	TGGACAAAGACACAATCACACA	TTGAATTCGATCTTTCCATCA
β -actin	CTGATGCAAAAAGTCCAAA	ACCGCACTCAAAGGTTCAAT

column (100 mm \times 2.1 mm, 1.7 m, Waters, United Kingdom). The temperature of the column oven was kept at 35°C. Solution A (25 mM ammonium acetate +25 mM NH₄H₂O) and Solution B were used as the mobile phase. The flow rate was 0.4 ml/min. The following were the gradient elution conditions: 95% B for the first 0.5 min; 95%–65% B for the next 0.5–9.5 min; 65%–40% B for the next 9.5–10.5 min; 40% B for the next 10.5–12 min; 40% B for the next 12–12.2 min; and 95% B for the next 12.2–15 min. Each sample received a 4 L injection. The metabolites eluted from the column were detected using a high-resolution tandem mass spectrometer TripleTOF5600plus (SCIEX, Cheshire, United Kingdom). Positive and negative ion modes of the Q-TOF were both utilized. The chromatograph and mass spectrometer were controlled by XCMS software 3.2.0 (UC, Berkeley, CA, United States).

2.6 Detection and evaluation of metabolite concentrations

The MSConvert software was utilized to convert raw LC-MS data into the mzXML format, which was further processed by the XCMS, CAMERA, and metaX toolboxes, which were all integrated within the R program (Li et al., 2018; Stanstrup et al., 2019). To identify each ion, the combined retention time (RT) and m/z data was utilized. The Plant Metabolic Pathway Databases (PLANTCYC; <http://www.plantcyc.org/>), Kyoto Encyclopedia of Genes and Genomes (KEGG; <http://www.kegg.jp/>), and Saskatoon Public Library in-House

Databases (<http://spldatabase.saskatoonlibrary.ca/>), and Human Metabolome Databases (HMDB; <http://www.hmdb.ca/>) were used to perform level-one and level-two identification and annotation to explain the physico-chemical properties as well as the biological functions of metabolites. The metaX software (<http://metax.genomics.cn/>), was employed for screening and quantitative analysis of differential metabolites.

2.7 Statistical analysis

The relative gene expressions were computed utilizing the 2^{- $\Delta\Delta$ CT} method (Livak and Schmittgen, 2001), and data visualization was performed utilizing GraphPad Prism 5 (GraphPad Software Inc., San Diego, California, United States). Both the heatmap and the cluster analyses were performed with the help of R-3.4.2 and MEGA6, respectively. For the analysis of significant differences, IBM SPSS (IBM SPSS Software Inc., San Diego, California, United States) was used.

3 Results

3.1 Flower color variation among *Camellia* genotypes

In attempt to understand the molecular mechanism underlying the color formation and differentiation in *C.*



FIGURE 1
Different flower colors among three *Camellia reticulata*. (A) *C. reticulata* (HHYC), (B) *C. reticulata* ‘Tongzimian’ (TZM), (C) *C. reticulata* ‘Xuejiao’ (XJ).

reticulata, we performed transcriptome and metabolome profiling of petals from *C. reticulata* (HHYC), *C. reticulata* ‘Xuejiao’ (XJ) and *C. reticulata* ‘Tongzimian’ (TZM). The petals of HHYC and TZM are red and white, respectively (Figures 1A,B), while the petals of XJ are the intermediate of HHYC and TZM, thus pink (red-white) color (Figure 1C).

3.2 Transcriptome profiling of petals from three contrasting flowers of *C. reticulata*

The transcriptome profiling was performed on nine libraries (3 genotypes) with contrasting petals/flowers \times 3 biological repeats leading to an average of 47, 49 and 48 Gb data for HHYC, XJ and TZM, respectively (Table 2). Of these, an average of 45,500,491 bp were clean reads with an error rate of 0.02% (Table 2). Furthermore, the Q30 (%) and guanine-cytosine content ranged from 94.55 to 95.15 and 44.51–45.30%, respectively (Table 2). These results suggest that the transcriptome results qualified for further downstream analyses.

In all, 61,277 genes comprising 44,751 known genes and 16,526 novel genes were detected from the nine libraries (Supplementary Table S1). From these, 53,861, 53,739 and 54,631 genes were expressed in HHYC, XJ and TZM, respectively. The fragments per kilobase of exon per million fragments mapped (FPKM) distribution and principal component analysis (PCA) of the expressed genes are shown in Figures 2A,B. The Pearson correlation coefficients ($r \geq 0.81$) and PCA based on FPKM showed high levels of reproducibility of petal samples from the same genotype (Supplementary Figure S1). Most of the expressed genes were successfully annotated to at

least one of the nine public databases, i.e., Kyoto Encyclopedia of Genes and Genomes (KEGG), KEGG pathway, NCBI non-redundant (NR), Swiss protein (Swissprot), KEGG orthologous (KOG), Gene ontology (GO), Protein family (Pfam) and Transcription factor (TF) family (Supplementary Table S1). The successful annotation of most of the identified genes coupled with high reproducibility and repeatability of petal samples from the same genotype give credence to our transcriptome results for the identification of differentially expressed genes (DEGs) and subsequent analyses.

3.4 Differentially expressed genes and Kyoto encyclopedia of genes and genomes pathway analyses

A total of 11,746 DEGs were detected among the HHYC, XJ and TZM genotypes in pairwise comparisons upon application of strict criteria of \log_2 fold change (\log_2FC) ≥ 1 and false discovery rate (FDR) with adjusted p -value ($padj$) < 0.05 . We subsequently performed hierarchical clustering heatmap of biological replicates from the three genotypes based on the FPKM values of the DEGs, the nine samples were divided into two major groups with each biological repeat in the sub-group. The two major groups comprised HHYC in group I, while XJ and TZM formed the group II (Figure 3A). The grouping pattern suggests that XJ and TZM have some level of similarity in terms of flower coloration mechanism (Figure 1). Among the pairwise groups, 6169, 7512 and 5134 DEGs were detected in HHYC_vs_XJ, HHYC_vs_TZM and XJ_vs_TZM, respectively (Supplementary Tables S2A-C;

TABLE 2 Summary of RNA-Seq data and mapping metrics of three contrasting flowers of *C. reticulata*.

Sample ^a	Raw reads (bp)	Clean reads (bp)	Clean base (Gb)	Error rate (%)	Reads mapped (%)	Unique mapped (%)	Q30 (%) ^b	GC (%) ^c
HHYC-1	48998284	47530980	7.13	0.02	75.54	71.12	94.90	45.30
HHYC-2	45727170	44108884	6.62	0.02	74.17	69.8	94.70	45.27
HHYC-3	48079296	42457662	6.37	0.02	73.58	69.03	94.81	45.28
HHYC	47601583	44699175	6.71	0.02	74.43	69.98	94.80	45.28
XJ-1	46926224	42171752	6.33	0.02	73.26	68.78	95.15	44.88
XJ-2	54057590	51492124	7.72	0.02	74.02	69.34	94.55	44.68
XJ-3	46145294	44832014	6.72	0.02	73.46	68.45	94.91	44.65
XJ	49043036	46165297	6.92	0.02	73.58	68.86	94.87	44.74
TZM-1	47604800	45981370	6.9	0.02	74.5	69.62	94.90	44.51
TZM-2	45923820	43484386	6.52	0.02	73.89	69.28	95.15	44.76
TZM-3	51788184	47445248	7.12	0.02	73.93	69.32	95.06	44.81
TZM	48438935	45637001	6.85	0.02	74.11	69.41	95.04	44.69
Average	48361185	45500491	6.83	0.02	74.04	69.42	94.90	44.90

^aSequencing was done in triplicate of *C. reticulata* (HHYC1-3), *C. reticulata* 'Xuejiao' (XJ1-3) and *C. reticulata* 'Tongziman' (TZM1-3), with HHYC, XJ, and TZM, representing the means.

^bQuality control at $\leq 30\%$.

^cGuanine and cytosine content.

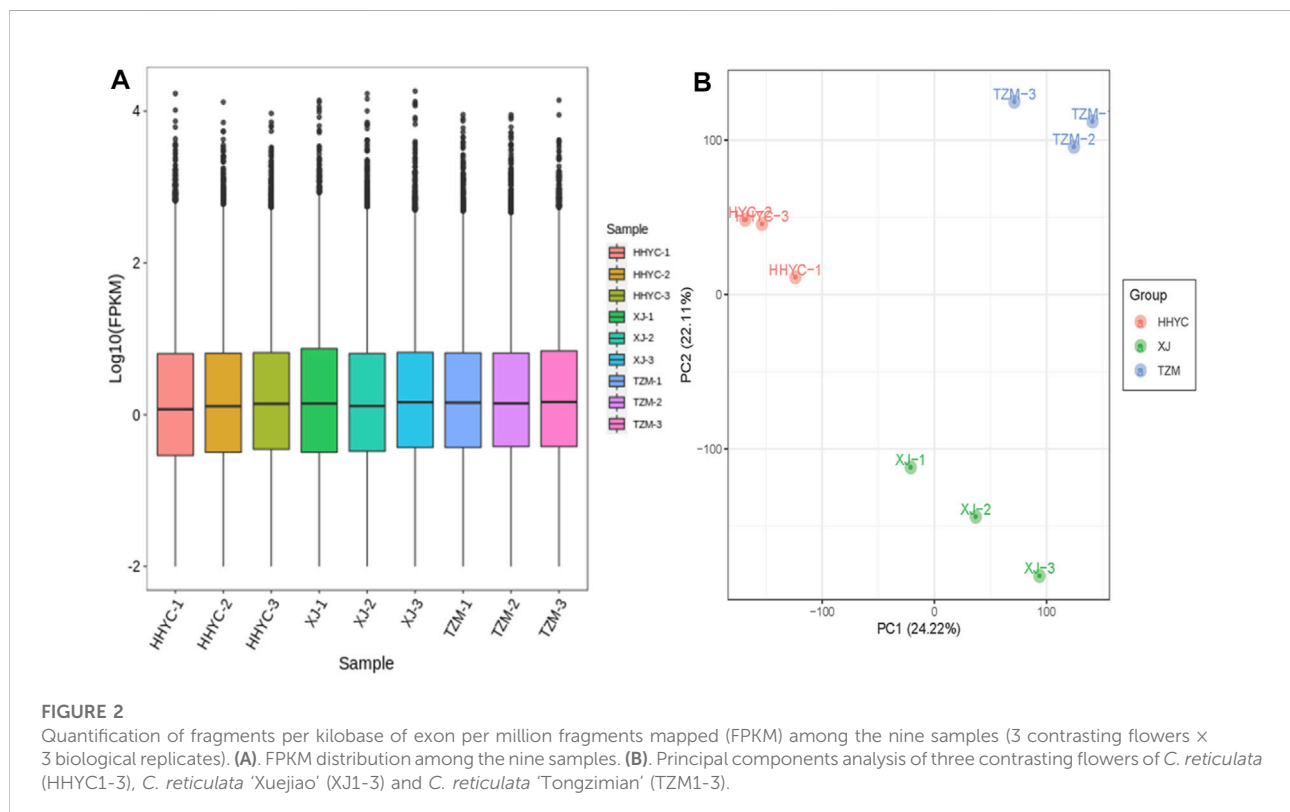
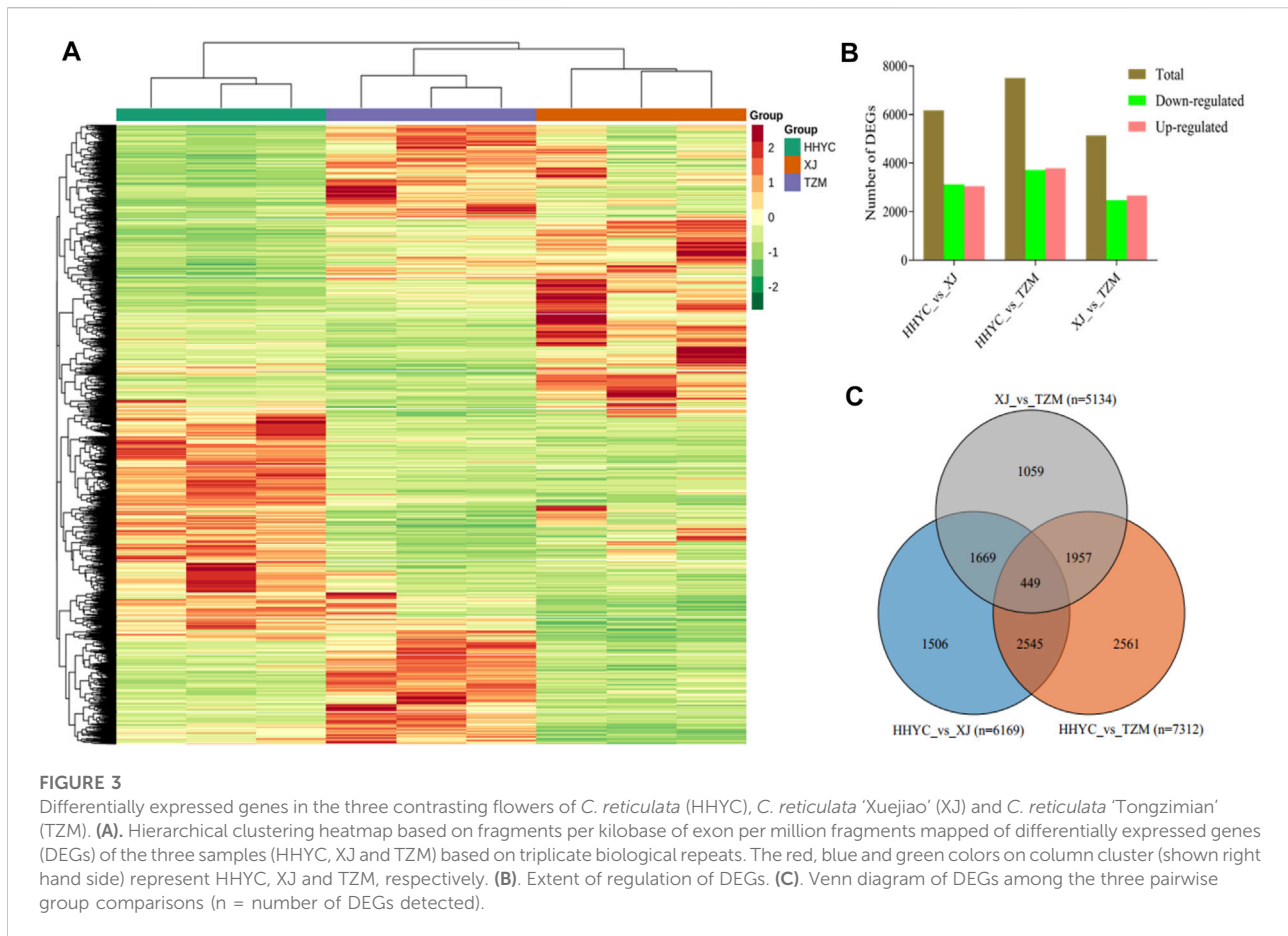


Figure 3B) with nearly equal proportion of up- and down-regulated genes. The least number of DEGs in XJ_vs_TZM further pinpoints the similarity in flower coloration mechanism. We also compared the results of DEGs in each

pairwise group and a total of 449 core conserved DEGs were detected among the three pairwise groups (Figure 3C). These results highlight that XJ and TZM have similar flower coloration mechanism than HHYC.



In order to verify the transcriptome results, 18 genes were randomly selected for qRT-PCR to establish the correlation between gene expression profiles from the RNA-seq and qRT-PCR. The relative expression levels of the selected genes were mostly consistent with that of RNA-seq with correlation score of 84% (Supplementary Figures S2A,B). This further confirms the reliability of transcript quantification from our RNA-seq.

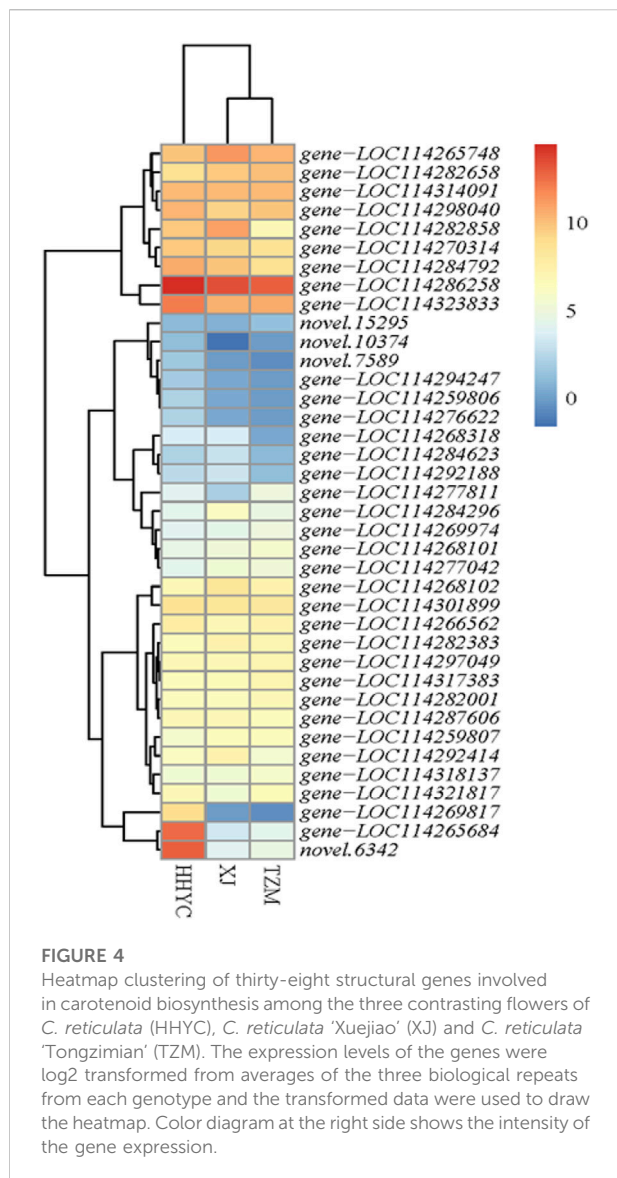
3.5 Analysis of key transcription factor families

It is well established that MYB-bHLH-WD40 (MBW) complex is involved in modulating coloration in plants (Fraser et al., 2013; Naik et al., 2021). However, in this study, no gene with WD40 was detected. Hence, we mined for MYB and bHLH transcription factors (TF) families among the DEGs and their log₂ transformed FPKM were heatmapped. A total of 276 and 174 genes with MYB and bHLH TFs were identified, respectively, from which 42 MYB and 29 bHLH were detected among the DEGs. We further studied the expression profiles of these genes (Supplementary Figure S3A,B). For instance, the expression of

gene-LOC114321352, *gene-LOC114268549*, *gene-LOC114264400* and *gene-LOC114281024* followed in HHYC or TZM were greater than XJ (Supplementary Figure S3A). In similar vein with rearrangement of the three genotypes by the 29 DEG encoding bHLH, *gene-LOC114233324*, *gene-LOC114258501*, *gene-LOC114298318*, *gene-LOC114287545* and *gene-LOC114319413* expressed lower in XJ relatively to either HHYC or TZM (Supplementary Figure S3A). The identified MYB-bHLH genes could be useful as genomic resources to deepen our understanding of transcriptional regulation flower coloration in *C. reticulata*.

3.6 Analysis of carotenoid biosynthetic pathway genes among three contrasting *C. reticulata* genotypes

Thirty-eight carotenoid biosynthetic structural genes were differentially expressed among the three pairwise groups. Their expression profiles were subjected to hierarchical clustering heatmap. The expression profiles of the 38 genes grouped the 3 genotypes of *C. reticulata* into 2 groups (Figure 4), just as the



hierarchical clustering heatmap of the 11,746 DEGs in Figure 3A. It is reported that carotenoid gives yellow-orange-red color to fruits/flowers in plants (Mortensen, 2006; Tanaka et al., 2008). Two ortholog genes (*gene-LOC114265684* and *novel.6342*) of *At4g38540* encoding for zeaxanthin epoxidase (ZEP) on the carotenoid biosynthetic pathway expressed more than 10-fold higher in HHYC than either XJ or TZM (Figure 4), suggesting these genes could be candidate genes for red pigmentation in HHYC. Several studies have demonstrated that ZEP is the major contributor to carotenoid composition (Gonzalez-Jorge et al., 2016; Lee et al., 2021). From the Figure 4, another gene worth elaborating is *gene-LOC114269817* encoding for abscisate beta-glucosyltransferase (ABA-UGT) [EC:2.4.1.263]. It was nearly not expressed in either XJ or TZM. This suggests that *gene-LOC114269817* may contribute to red coloration in HHYC as a recent study by Li et al. (2022) revealed that increase in ABA-

UGT gene contributed to red coloration in strawberry fruit, but its reduction contributed to white coloration in an unripe fruit.

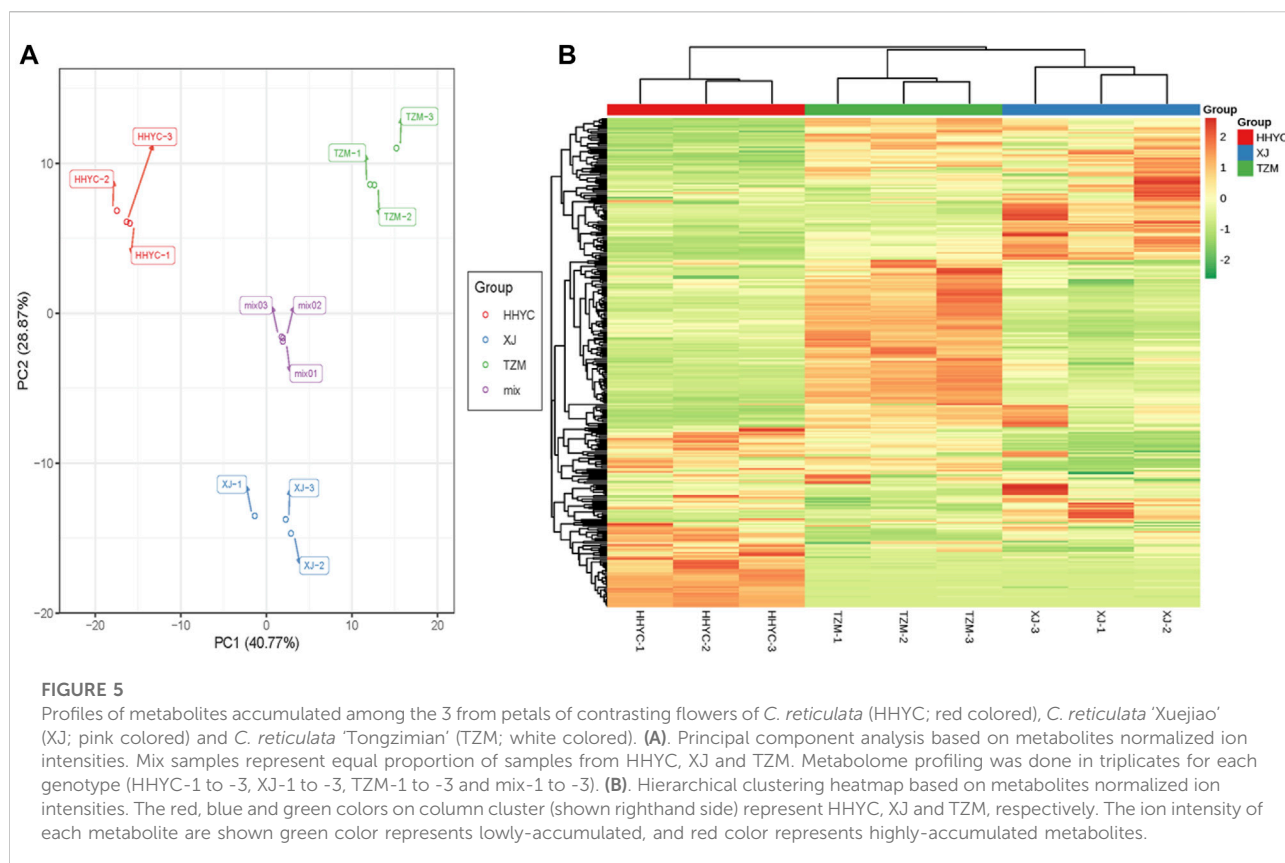
3.7 Analysis of phenylpropanoid/flavonoid/anthocyanin biosynthetic pathways genes among the three contrasting *C. reticulata* genotypes

Aside carotenoid biosynthesis, it is well known that flavonoids are major molecules involved in plant pigmentation specifically anthocyanins (Lai et al., 2014). Phenylpropanoids are precursors of flavonoid/flavone and flavonol which lead to anthocyanins biosynthesis and accumulation. Therefore, we explored DEGs in the pairwise groups based on the KEGG pathway enrichment analyses (Supplementary Table S3). Sixteen structural genes involved in flavone and flavonol biosynthesis (Ko0094) were differentially expressed between HHYC and XJ (Supplementary Table S2A). Out of these 16 structural genes, *gene-LOC114309343* (flavonoid 3'-monooxygenase [EC:1.14.14.82]) and other 2 genes (*gene-LOC114273964* and *gene-LOC114273955*) encoding flavonol-3-O-glucoside/galactoside glucosyltransferase and anthocyanidin 3-O-glucoside 2''-O-glucosyltransferase-like, were not expressed in XJ genotype, making them potential candidate genes for the white pigmentation in XJ.

Flavonoid biosynthesis (Ko00941) was enriched with 76 (45 down-regulated and 31 up-regulated) and 40 (25 down-regulated and 15 up-regulated) DEGs in HHYC_vs_TZM and XJ_vs_TZM, respectively (Supplementary Tables S2, 3). The higher number of down-regulated genes indicate that flavonoid biosynthetic genes were more activated in colored petals than the white petals (Figure 1). Additionally, anthocyanins biosynthesis was enriched with four DEGs (*gene-LOC114289234*, *gene-LOC114285765*, *gene-LOC114285774* and *gene-LOC114288492*) encoding anthocyanidin 3-O-glucosyltransferase [EC:2.4.1.115]. The DEGs were expressed higher (2.22–18.14 times) in HHYC than in TZM (Supplementary Table S2A). Likewise, these genes expressed higher in XJ genotype than in TZM genotype (Supplementary Table S2A). These suggest that the weak expression of anthocyanidin 3-O-glucosyltransferase encoded genes are likely responsible for the white flower coloration in TZM genotype. These genes are involved in the conversion of pelargonidin, cyanidin and delphinidin to pelargonidin 3-glucoside, cyanidin 3-glucoside and delphinidin 3-glucoside, respectively (Supplementary Figures S4A,B).

3.8 Flavonoid-based metabolome profiling of flowers of the three contrasting *C. reticulata*

To further understand the metabolites involved in the reddish color formation in HHYC compared to the two other



genotypes, we performed a targeted metabolome profiling of flavonoid compounds in the three genotypes. This led to a total of 310 metabolites (282 flavonoids and 28 tannins) detected (Supplementary Table S4). We performed PCA and hierarchical heatmap clustering based on the ion intensities of the 310 compounds. We observed that the grouping/topology (Figures 5A,B) followed the FKPM of genes obtained from the RNA-seq (Figure 3A).

To identify the differentially accumulated metabolites (DAMs), we performed partial least squares discriminant analysis (PLS-DA) with threshold of $\log_2FC \geq 1$ and variable importance in projection (VIP) ≥ 1 . From these stringent criteria, we detected 138, 149 and 133 DAMs in HHYC_vs_XJ, HHYC_vs_TZM and XJ_vs_TZM, respectively (Supplementary Figures S5A,B; Supplementary Table S5).

From above, 18 anthocyanin-based DAMs were detected with an accumulation pattern: HHYC > XJ > TZM (Table 3). All the 18 DAMs were detected in HHYC, while only nine and seven DAMs were detected in XJ and TZM genotypes, respectively. These trends suggest that anthocyanin is the major pigment responsible for the flower coloration among the three contrasting genotypes of *C. reticulata*. For instance, cyanidin 3-xyloside (Hmhp002834), cyanidin-3,5-O-diglucoside (cyanin) (pme1777),

cyanidin-3-O-(6''-O-malonyl)glucoside (pmb0542), cyanidin-3-O-arabinoside (Smlp002532), cyanidin-3-O-galactoside (pmf0027), cyanidin-3-O-glucoside (kuromanin) (pmb0550), cyanidin-3-O-rutinoside (keracyanin) (pme1773), delphinidin-3,5-di-O-glucoside (pmf0116), delphinidin-3-O-arabinoside (Smlp001915), delphinidin-3-O-galactoside (Lmcp001821), delphinidin-3-O-glucoside (mirtillin) (pme1398), delphinidin-3-O-sophoroside-5-O-glucoside (Lmqp001553), pelargonidin-3-O-glucoside (pme3392), peonidin-3-O-(6''-O-p-coumaroyl)glucoside (Lmpp003929) and peonidin-3-O-glucoside (pmf0203) accumulated higher in HHYC genotype but were either completely absent or lower in either XJ or TZM (Table 3).

On the contrary, cyanidin-3-O-(6''-O-caffeoyl-2''-O-xylosyl) glucoside (Lmcp004347) and cyanidin-3-O-(6''-O-p-coumaroyl-2''-O-xylosyl) glucoside (Lmjp002491) accumulated higher in XJ than in HHYC and TZM (Table 3), making candidate biomarkers to distinguish flowers of the three genotypes. The complete absence of cyanidin 3-xyloside (Hmhp002834), cyanidin-3-O-(6'''-O-acetyl-2'''-O-xylosyl) glucoside (Lmcp003751), cyanidin-3-O-arabinoside (Smlp002532) and cyanidin-3-O-galactoside (pmf0027) in TZM may be responsible for the flower color differentiation between XJ and TZM genotypes.

TABLE 3 Ion intensities of anthocyanin-based differentially accumulated metabolites among petals from three contrasting flowers of *C. reticulata*.

Index ^a	Compounds	HHYC ^b	XJ ^c	TZM ^d
Hmhp002834	Cyanidin 3-xyloside	27941333	24756	Absent
pme1777	Cyanidin-3,5-O-diglucoside (Cyanin)	30024333	36218	111577
Lmcp003751	Cyanidin-3-O-(6'''-O-acetyl-2'''-O-xylosyl) glucoside	6382	277067	Absent
Lmcp004347	Cyanidin-3-O-(6''-O-caffeoyl-2''-O-xylosyl) glucoside	38132	3406100	241843
pmb0542	Cyanidin-3-O-(6''-O-malonyl) glucoside	360783	Absent	Absent
Lmjp002491	Cyanidin-3-O-(6''-O-p-coumaroyl-2''-O-xylosyl) glucoside	771273	28742000	12310900
Smlp002532	Cyanidin-3-O-arabinoside	30060333	15886	Absent
pmf0027	Cyanidin-3-O-galactoside	13049667	28850	Absent
pmb0550	Cyanidin-3-O-glucoside (Kuromanin)	15752000	Absent	Absent
pme1773	Cyanidin-3-O-rutinoside (Keracyanin)	2957200	Absent	Absent
pmf0116	Delphinidin-3,5-di-O-glucoside	4171133	11328	37114
Smlp001915	Delphinidin-3-O-arabinoside	207653	Absent	Absent
Lmcp001821	Delphinidin-3-O-galactoside	18885000	Absent	158770
pme1398	Delphinidin-3-O-glucoside (Mirtillin)	18257667	Absent	145603
Lmqp001553	Delphinidin-3-O-sophoroside-5-O-glucoside	23826	Absent	Absent
pme3392	Pelargonidin-3-O-glucoside	22014000	Absent	Absent
Lmpp003929	Peonidin-3-O-(6''-O-p-coumaroyl) glucoside	1275933	29948	19105
pmf0203	Peonidin-3-O-glucoside	11068667	Absent	Absent
Average		10,936,962.05	3,619,128.11	1,860,701.81

^aCompound index from self-built database MWDB (Metware database).

^b*C. reticulata* (HHYC).

^c*C. reticulata* 'Xuejiao' (XJ). *C. reticulata* 'Tongzimian' (TZM). Ion intensities were computed as the average of the three biological repeats of each genotype.

3.9 Conjoint analysis of transcriptome and metabolome results

We further performed a conjoint analysis of the transcriptome and metabolome data to assess the relationship between the genes and metabolites. This helps to statistically prioritize genes and metabolites that alter flower colors in *C. reticulata*. It was observed that anthocyanin is the key pigmentation that differentiates flowers of HHYC_vs_XJ and HHYC_vs_TZM ($p = 0.004$), however XJ_vs_TZM were not differentiated, possibly as a result of high similarity between the flowers of XJ and TZM as observed in the heatmap clustering (Figure 3A; Figure 5B; Figure 6).

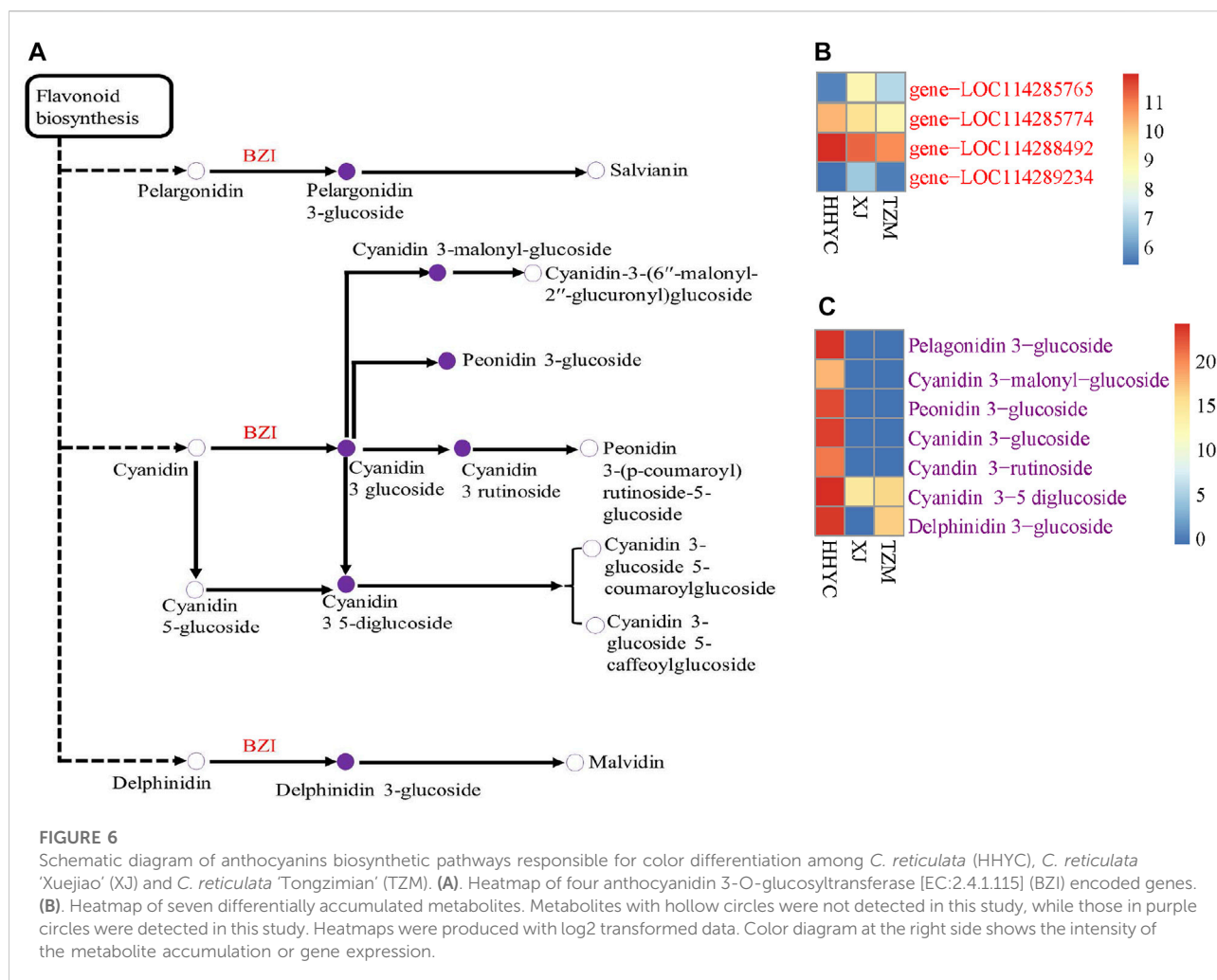
A total of two DEGs (*gene-LOC114285765* and *gene-LOC114289234*) encoding for anthocyanidin 3-O-glucosyltransferase [EC:2.4.1.115] (BZI) were identified to associate (Pearson's correlation >0.80) with seven DAMs (pme3392 (Pelargonidin-3-O-glucoside), pmb0550 (cyanidin-3-O-glucoside (Kuromanin)), pmf0203 (peonidin-3-O-glucoside), pmb0542 (cyanidin-3-O-(6''-O-malonyl)glucoside), pme1773 (cyanidin-3-O-rutinoside (keracyanin)), pme1777 (cyanidin-3,5-O-diglucoside cyanin) and pmf0116 (delphinidin-3,5-di-O-glucoside)) in both HHYC_vs_XJ and HHYC_vs_TZM (Figures 7A–C). The two genes expressed higher in HHYC than either XJ or TZM. BZI genes are responsible for the conversion of pelargonidin, cyanidin and

delphinidin to pelargonidin 3-glucoside, cyanidin 3-glucoside and delphinidin 3-glucoside, respectively. Among the seven DAMs, only pme1777 (cyanidin-3,5-O-diglucoside cyanin) and pmf0116 (delphinidin-3,5-di-O-glucoside) accumulated lower in either XJ or TZM than in HHYC, while the remaining five were completely absent in both XJ and TZM (Figures 7A–C).

4 Discussion

Flower color is one of the most important features of horticultural crops, including *C. reticulata* (Xin et al., 2015). It does not only affect economic value, but eye appeal, aesthetics and quality. With more than 500 cultivars of *C. reticulata* with diverse flower color phenotypes (Xin et al., 2015), the regulatory mechanism underlying flower coloration among the cultivars remain unknown.

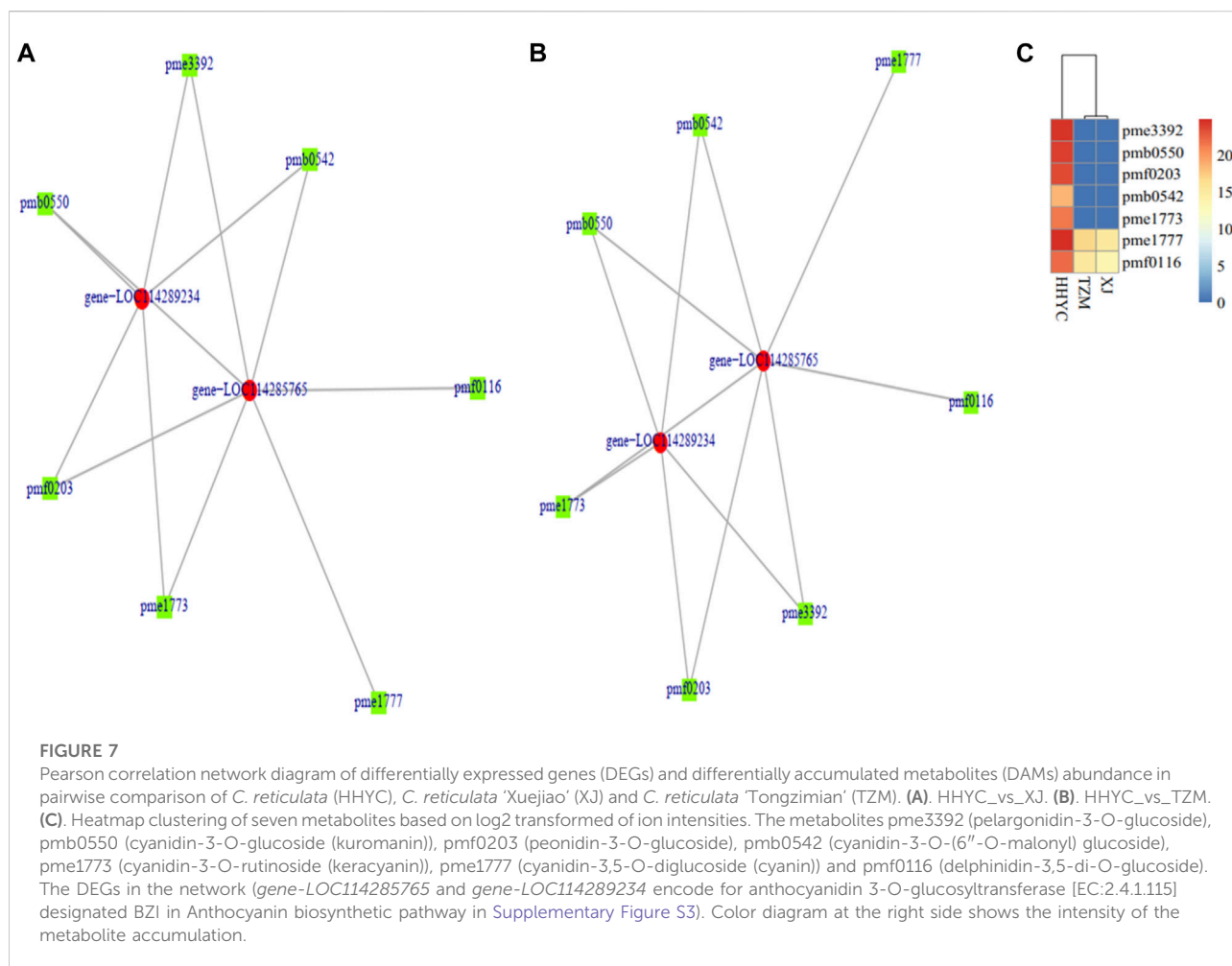
Flavonoid/anthocyanins, betalains, carotenoids and chlorophylls are well known to modulate color pigmentation in plants (Mortensen, 2006; Tanaka et al., 2008; Lai et al., 2014; Zhao et al., 2017; Shen et al., 2019). With exception of chlorophylls, the other three pigmentations have been elucidated to regulate color variation depending on their synthesis, structures and subcellular localization (Zhao and Tao, 2015). Carotenoids are well documented to confer



yellow, orange and red colorations (Shen et al., 2019), while anthocyanins are responsible for blue, purple, red or white colorations (Yan and Kerr, 2013). The transcriptome profile from the flowers with red, white and intermediate (pink) genotypes (HHYC, XJ and TZM, respectively) revealed that carotenoids and anthocyanins (Supplementary Table S3) co-exist which were pronounced in the red flower genotype (HHYC) (Figure 1). For instance, two ZEP genes (*gene-LOC114265684* and *novel.6342*) and one ABA-UGT (*gene-LOC114269817*) (Figure 4) involved in carotenoid biosynthesis as well as flavonoids/anthocyanins structural genes (Supplementary Table S2) including three anthocyanidin 3-O-glucosyltransferase (*gene-LOC114289234*, *gene-LOC114285765*, *gene-LOC114285774* and *gene-LOC114288492*) expressed higher in the HHYC genotype than XJ and TZM genotypes. These results highlight the co-regulation of red flower color in HHYC genotype by anthocyanins and carotenoids, with a least contribution of the latter. Our findings are consistent with the findings of Li et al. (2022); Xue et al. (2016). In addition, down-regulation/absence of anthocyanidin 3-O-glucosyltransferase is

responsible for inhibition of the synthesis of delphinidin 3-glucoside (Takeda et al., 1990; Yabuya et al., 2002; Muhammad et al., 2022) and Yamazaki et al. (1999) and Nakatsuka et al. (2008) reported that a reduced level of delphinidin limits red coloration. The absence/down-regulation of anthocyanidin 3-O-glucosyltransferase genes in XJ or TZM implies that late stage of anthocyanins biosynthesis may have been blocked (Lai et al., 2013). The two ZEP genes (*gene-LOC114265684* and *novel.6342*), one ABA-UGT (*gene-LOC114269817*) and three anthocyanidin 3-O-glucosyltransferase (*gene-LOC114289234*, *gene-LOC114285765*, *gene-LOC114285774* and *gene-LOC114288492*) could be targeted to study the structural variation which is responsible for color variation between XJ and TZM. There are reports that nucleotide variation in structural genes involved in anthocyanin biosynthesis could cause variations in coloration in some plants (Ben-Simhon et al., 2015).

Transcription factors are proteins involved in converting, or transcribing DNA into RNA. It is well established the involvement of MYB-bHLH-WD40 (MBW) complex in modulating coloration



in plants (Li et al., 2020a; Naik et al., 2021). Among the 61,277 expressed genes including 44,751 known genes and 16,526 novel genes were detected in the present study, no WD40 structural gene was found (Supplementary Table S1). Four MYB transcription factor genes (*gene-LOC114321352*, *gene-LOC114268549*, *gene-LOC114264400* and *gene-LOC114281024*) and four bHLH genes (*gene-LOC114233324*, *gene-LOC114258501*, *gene-LOC114298318*, *gene-LOC114287545* and *gene-LOC114319413*) expressed higher in genotypes with red color (either HHYC or TZM) than in the white pigmented genotype, XJ (Supplementary Figure S3). These suggest that MYB and bHLH transcription factors are potential positive regulators of carotenoid and anthocyanin biosynthesis in *C. reticulata*. Zhou et al. (2019) revealed that *CpbHLH1/2* modulates carotenoid biosynthesis-related genes in papaya, while He et al. (2022) demonstrated that *UpMYB44* controls carotenoid biosynthesis-related genes in *Ulva prolifera*. In comparison with other crops, MYB-bHLH role in regulating carotenoid and anthocyanin biosynthesis needs to be unearthed with genes reported in this study (Ramsay and Glover, 2005; Gonzalez et al., 2008; Zhao et al., 2012). It is important to link the identified

key TFs to the target structural genes involved in the synthesis of anthocyanins through gene co-expression analysis. Such analysis will require more transcriptome data, which could be the subject of a further study.

We further performed targeted metabolome profiling with the petals of three contrasting genotypes of *C. reticulata* with the aim of identifying specific flavonoid/anthocyanin compound(s) that may account for white coloration observed in XJ and TZM genotypes relative to HHYC genotype. Targeted metabolome profiling offers absolute quantification, higher accuracy, and greater selectivity (Beckles and Roessner, 2012; Cao et al., 2020; Lelli et al., 2021). From this, 310 metabolites comprising 282 and 28 flavonoid/anthocyanin and tannin compounds, were detected, respectively (Supplementary Table S4). These compounds mostly accumulated higher in either HHYC or TZM genotype than in XJ genotype (Supplementary Table S4). For example, Luteolin-7-O-gentiobioside which is flavone compound accumulated in order of HHYC (61,965,667) > TZM (1,657,300), but was completely absent in XJ. This compound is reported to cause pink coloration in *Myoporum bontioides* (Myoporaceae) (Iwashina and Kokubugata,

2014; Cao et al., 2020). In all, eighteen anthocyanin compounds were detected among the three contrasting genotypes with wide variation in flower colors (Table 3). Of these, only 9 and 7 compounds were detected in XJ and TZM genotypes, respectively. The absence/presence of some anthocyanin compounds could be the basis for color differentiation among the three genotypes of *C. reticulata*. Cyanidin, a major anthocyanin compound which accounts for red coloration had 8 derivatives compounds (cyanidin-3-O-(6"-O-malonyl) glucoside, cyanidin-3-O-(6"-O-p-coumaroyl-2"-O-xylosyl) glucoside, cyanidin-3-O-arabinoside, cyanidin-3-O-galactoside, cyanidin-3-O-glucoside (kuromanin), and cyanidin-3-O-rutinoside (keracyanin). Of these, cyanidin-3-O-glucoside, and cyanidin-3-O-rutinoside were exclusively detected in HHYC genotype which is consistent with the findings of Kim and Kokubugata (2010) who found these compounds in red pigmented flower cultivar of buckwheat (Gan-Chao), but were absent in the white-flowered cultivar (Tanno). In another study, Li et al. (2020b) found delphinidin 3-O-rutinoside and petunidin 3-O-glucoside to be absent in white fruit of *Lycium ruthenicum* Murray. Similar observations were made among the white, violet and red flowers of *Rhododendron schlippenbachii* Maxim (Kim et al., 2013). All these indicate that the absence and reduction of anthocyanin compounds could account for the white and pink (red-white) flower coloration in XJ and TZM, respectively.

In summary, this study provides important insights into flower coloration in *C. reticulata* by unearthing key structural genes and transcription factors. This forms a foundation for biotechnological applications to explore their regulatory mechanisms in flower coloration (Kim et al., 2013; Varshney et al., 2020, 2021). Also, the flavonoid/anthocyanin compounds identified in this study could be validated and used to develop biomarkers for metabolome-assisted breeding programs (Varshney et al., 2020; Jamaloddin et al., 2021).

Data availability statement

The data presented in this study are deposited in the National Genomic Data Center under the accession number PRJCA012977 (<https://ngdc.cnbc.ac.cn/search/?dbld=&q=PRJCA012977>).

Author contributions

FG, RN, and LC designed the experiments. FG, RN, YH, and SC performed the experiments. FG, RN, NY, LC, and XC analyzed the data. FG and RN wrote the manuscript. FG, NY, LC, ST, and LQC revised the manuscript. All authors read and approved the final version of the manuscript.

Funding

This research is supported by the national "13th Five-Year Plan" key research and development plan project "Flower Efficient Breeding Technology and Variety Creation (2019YFD1001000)" Project 05: "Camellia Efficient Breeding Technology and Variety Creation (2019YFD100100005)" sub-project "Yunnan Camellia Efficient Breeding Technology and Variety" Created (2019YFD100005-2)" and the Yunnan Provincial Agricultural Basic Research Joint Special Project "Mining and functional research on key genes for the formation of white flowers in Dianshan tea (202101BD070001-095)", National Key R&D Program of China (2019YFD1001000), Yunnan agricultural basic research joint special general project (202101BD070001-095), and the Outstanding Young Talents Support Program of Yunnan Province (YNWR-QNBJ-2019-280). Funders have no role in the design and publication of the manuscript.

Acknowledgments

We thank Yunlong Wu, Yongming Shi, Jianping Jiao, Xueqin Wu, Xueyan Chi, and members of Camellia groups for their technical support and stimulating discussions.

Conflict of interest

The authors declare that the research was conducted in the absence of any commercial or financial relationships that could be construed as a potential conflict of interest.

Publisher's note

All claims expressed in this article are solely those of the authors and do not necessarily represent those of their affiliated organizations, or those of the publisher, the editors and the reviewers. Any product that may be evaluated in this article, or claim that may be made by its manufacturer, is not guaranteed or endorsed by the publisher.

Supplementary material

The Supplementary Material for this article can be found online at: <https://www.frontiersin.org/articles/10.3389/fgene.2022.1059717/full#supplementary-material>

References

- Allan, A. C., Hellens, R. P., and Laing, W. A. (2008). MYB transcription factors that colour our fruit. *Trends Plant Sci.* 13, 99–102. doi:10.1016/j.tplants.2007.11.012
- Anders, S. (2010). Analysing RNA-Seq data with the DESeq package. *Mol. Biol.* 43, 1–17.
- Beckles, D. M., and Roessner, A. (2012). Plant metabolomics: Applications and opportunities for agricultural biotechnology. *Plant Biotechnol. Agric.*, 67–81. doi:10.1016/B978-0-12-381466-1.00005-5
- Ben-Simhon, Z., Judeinstein, S., Trainin, T., Harel-Beja, R., Bar-Yaakov, I., Borochoy-Neori, H., et al. (2015). A “white” anthocyanin-less pomegranate (*Punica granatum* L.) caused by an insertion in the coding region of the leucoanthocyanidin dioxygenase (LDOX; ANS) gene. *PLoS One* 10, e0142777. doi:10.1371/journal.pone.0142777
- Benjamini, Y., and Hochberg, Y. (1995). Controlling the false discovery rate: A practical and powerful approach to multiple testing. *J. R. Stat. Soc. Ser. B* 57, 289–300. doi:10.1111/j.2517-6161.1995.tb02031.x
- Cao, G., Song, Z., Hong, Y., Yang, Z., Song, Y., Chen, Z., et al. (2020). Large-scale targeted metabolomics method for metabolite profiling of human samples. *Anal. Chim. Acta* 1125, 144–151. doi:10.1016/j.aca.2020.05.053
- Chen, S. M., Li, C. H., Zhu, X. R., Deng, Y. M., Sun, W., Wang, L. S., et al. (2012). The identification of flavonoids and the expression of genes of anthocyanin biosynthesis in the chrysanthemum flowers. *Biol. Plant.* 56, 458–464. doi:10.1007/S10535-012-0069-3
- Cloutault, J., Peltier, D., Berruyer, R., Thomas, M., Briard, M., and Geoffriau, E. (2008). Expression of carotenoid biosynthesis genes during carrot root development. *J. Exp. Bot.* 59, 3563–3573. doi:10.1093/jxb/ERN210
- Cui, D., Zhao, S., Xu, H., Allan, A. C., Zhang, X., Fan, L., et al. (2021). The interaction of MYB, bHLH and WD40 transcription factors in red pear (*Pyrus pyrifolia*) peel. *Plant Mol. Biol.* 106, 407–417. doi:10.1007/S11103-021-01160-W
- Escribano-Bailon, M. Y., and Santos-Buelga, C. (2012). Anthocyanin copigmentation – evaluation, mechanisms and implications for the colour of red wines. *Curr. Org. Chem.* 16, 715–723. doi:10.2174/138527212799957977
- Feng, F., Li, M., Ma, F., and Cheng, L. (2013). Phenylpropanoid metabolites and expression of key genes involved in anthocyanin biosynthesis in the shaded peel of apple fruit in response to sun exposure. *Plant Physiol. biochem.* 69, 54–61. doi:10.1016/j.plaphy.2013.04.020
- Fraser, L. G., Seal, A. G., Montefiori, M., McGhie, T. K., Tsang, G. K., Datson, P. M., et al. (2013). An R2R3 MYB transcription factor determines red petal colour in an Actinidia (kiwifruit) hybrid population. *BMC Genomics* 14, 28. doi:10.1186/1471-2164-14-28
- Gao, Y. F., Zhao, D. H., Zhang, J. Q., Chen, J. S., Li, J. L., Weng, Z., et al. (2021). De novo transcriptome sequencing and anthocyanin metabolite analysis reveals leaf color of *Acer pseudosibiricum* in autumn. *BMC Genomics* 22, 383–412. doi:10.1186/s12864-021-07715-x
- Gonzalez, A., Zhao, M., Leavitt, J. M., and Lloyd, A. M. (2008). Regulation of the anthocyanin biosynthetic pathway by the TTG1/bHLH/Myb transcriptional complex in Arabidopsis seedlings. *Plant J.* 53, 814–827. doi:10.1111/j.1365-3113.2007.03373.X
- Gonzalez-Jorge, S., Mehrshahi, P., Magallanes-Lundback, M., Lipka, A. E., Angelovici, R., Gore, M. A., et al. (2016). Zeaxanthin epoxidase activity potentiates carotenoid degradation in maturing seed. *Plant Physiol.* 171, 1837–1851. doi:10.1104/PP.16.00604
- He, J., and Giusti, M. (2010). Anthocyanins: Natural colorants with health-promoting properties. *Annu. Rev. Food Sci. Technol.* 1, 163–187. doi:10.1146/annurev.food.080708.100754
- He, Y., Li, M., Wang, Y., and Shen, S. (2022). The R2R3-MYB transcription factor MYB44 modulates carotenoid biosynthesis in *Ulva prolifera*. *Algal Res.* 62, 102578. doi:10.1016/j.algal.2021.102578
- Hichri, I., Barrieu, F., Bogs, J., Kappel, C., Delrot, S., and Lauvegeat, V. (2011). Recent advances in the transcriptional regulation of the flavonoid biosynthetic pathway. *J. Exp. Bot.* 62, 2465–2483. doi:10.1093/jxb/ERQ442
- Hu, J., Chen, G., Zhang, Y., Cui, B., Yin, W., Yu, X., et al. (2015). Anthocyanin composition and expression analysis of anthocyanin biosynthetic genes in kidney bean pod. *Plant Physiol. biochem.* 97, 304–312. doi:10.1016/j.plaphy.2015.10.019
- Iwashina, T., and Kokubugata, G. (2014). Flavonoids from the flowers and aerial parts of *toronia concolor* var. *formosana*. *Bull. Natl. Mus. Nat. Sci. Ser. B* 40, 55–59.
- Jamaloddin, M., Maliha, A., Gokulan, C. G., Gaur, N., and Patel, H. K. (2021). Metabolomics-assisted breeding for crop improvement: An emerging approach. *Omi. Technol. Sustain. Agric. Glob. Food Secur.* 1, 241–279. doi:10.1007/978-981-16-0831-5_11
- Jiang, S., Sun, Q., Zhang, T., Liu, W., Wang, N., and Chen, X. (2021). MdMYB114 regulates anthocyanin biosynthesis and functions downstream of MdbZIP4-like in apple fruit. *J. Plant Physiol.* 257, 153353. doi:10.1016/j.jplph.2020.153353
- Joshi, R., and Gulati, A. (2011). Biochemical attributes of tea flowers (*Camellia sinensis*) at different developmental stages in the Kangra region of India. *Sci. Hortic. Amst.* 130, 266–274. doi:10.1016/j.scienta.2011.06.007
- Kim, Y. B., Park, S. Y., Thwe, A. A., Seo, J. M., Suzuki, T., Kim, S. J., et al. (2013). Metabolomic analysis and differential expression of anthocyanin biosynthetic genes in white- and red-flowered buckwheat cultivars (*Fagopyrum esculentum*). *J. Agric. Food Chem.* 61, 10525–10533. doi:10.1021/jf402258f
- Lai, B., Li, X. J., Hu, B., Qin, Y. H., Huang, X. M., Wang, H. C., et al. (2014). LcMYB1 is a key determinant of differential anthocyanin accumulation among genotypes, tissues, developmental phases and ABA and light stimuli in litchi chinensis. *PLoS One* 9, e86293. doi:10.1371/journal.pone.0086293
- Lai, Y., Li, H., and Yamagishi, M. (2013). A review of target gene specificity of flavonoid R2R3-MYB transcription factors and a discussion of factors contributing to the target gene selectivity. *Front. Biol.* 86 (8), 577–598. doi:10.1007/S11515-013-1281-Z
- Lee, S. Y., Jang, S. J., Jeong, H. B., Lee, S. Y., Venkatesh, J., Lee, J. H., et al. (2021). A mutation in Zeaxanthin epoxidase contributes to orange coloration and alters carotenoid contents in pepper fruit (*Capsicum annuum*). *Plant J.* 106, 1692–1707. doi:10.1111/TPJ.15264
- Lelli, V., Belardo, A., and Maria Timperio, A. (2021). From targeted quantification to untargeted metabolomics. *Metabolomics - Methodol. Appl. Med. Sci. Life Sci.* doi:10.5772/INTECHOPEN.96852
- Li, B.-J., Grierson, D., Shi, Y., and Chen, K.-S. (2022). Roles of abscisic acid in regulating ripening and quality of strawberry, a model non-climacteric fruit. *Hortic. Res.* 9. doi:10.1093/HR/UHAC089
- Li, H., Yang, Z., Zeng, Q., Wang, S., Luo, Y., Huang, Y., et al. (2020a2020). Abnormal expression of bHLH3 disrupts a flavonoid homeostasis network, causing differences in pigment composition among mulberry fruits. *Hortic. Res.* 7, 83–19. doi:10.1038/s41438-020-0302-8
- Li, J. B., Hashimoto, F., Shimizu, K., and Sakata, Y. (2013). Chemical taxonomy of red-flowered wild *Camellia* species based on floral anthocyanins. *Phytochemistry* 85, 99–106. doi:10.1016/j.phytochem.2012.09.004
- Li, T., Fan, Y., Qin, H., Dai, G., Li, G., Li, Y., et al. (2020b). Transcriptome and flavonoids metabolomic analysis identifies regulatory networks and hub genes in black and white fruits of *Lycium ruthenicum murrayi*. *Front. Plant Sci.* 11, 1256. doi:10.3389/fpls.2020.01256
- Li, Y., Fang, J., Qi, X., Lin, M., Zhong, Y., Sun, L., et al. (2018). Combined analysis of the fruit metabolome and transcriptome reveals candidate genes involved in flavonoid biosynthesis in *Actinidia arguta*. *Int. J. Mol. Sci.* 19, 1471. doi:10.3390/ijms19051471
- Livak, K. J., and Schmittgen, T. D. (2001). Analysis of relative gene expression data using real-time quantitative PCR and the 2⁻(Delta Delta C(T)) Method. *Methods* 25, 402–408. doi:10.1006/METH.2001.1262
- Lou, Q., Liu, Y., Qi, Y., Jiao, S., Tian, F., Jiang, L., et al. (2014). Transcriptome sequencing and metabolite analysis reveals the role of delphinidin metabolism in flower colour in grape hyacinth. *J. Exp. Bot.* 65, 3157–3164. doi:10.1093/jxb/ERU168
- Ma, K. F., Zhang, Q. X., Cheng, T. R., Yan, X. L., Pan, H. T., and Wang, J. (2018). Substantial epigenetic variation causing flower color chimerism in the ornamental tree *Prunus mume* revealed by single base resolution methylome detection and transcriptome sequencing. *Int. J. Mol. Sci.* 19 (19), 2315. doi:10.3390/ijms19082315
- Medda, S., Sanchez-Ballesta, M. T., Romero, I., Dessena, L., and Mulas, M. (2021). Expression of structural flavonoid biosynthesis genes in dark-blue and white myrtle berries (*Myrtus communis* L.). *Plants* 10, 316–16. doi:10.3390/PLANTS10020316
- Mei, X., Wan, S., Lin, C., Zhou, C., Hu, L., Deng, C., et al. (2021). Integration of metabolome and transcriptome reveals the relationship of benzenoid-phenylpropanoid pigment and aroma in purple tea flowers. *Front. Plant Sci.* 12, 2601. doi:10.3389/fpls.2021.762330
- Mekapogu, M., Vasamsetti, B. M. K., Kwon, O. K., Ahn, M. S., Lim, S. H., and Jung, J. A. (2020). Anthocyanins in floral colors: Biosynthesis and regulation in *Chrysanthemum* flowers. *Int. J. Mol. Sci.* 21, 65377–E6624. doi:10.3390/ijms21186537
- Mortensen, A. (2006). Carotenoids and other pigments as natural colorants. *Pure Appl. Chem.* 78, 1477–1491. doi:10.1351/pac200678081477
- Muhammad, N., Luo, Z., Yang, M., Li, X., Liu, Z., and Liu, M. (2022). The joint role of the late anthocyanin biosynthetic UFGT-encoding genes in the flowers and

- fruits coloration of horticultural plants. *Sci. Hortic.* 301, 111110. doi:10.1016/J.SCIENTA.2022.111110
- Naik, J., Rajput, R., Pucker, B., Stracke, R., and Pandey, A. (2021). The R2R3-MYB transcription factor *MtMYB134* orchestrates flavonol biosynthesis in *Medicago truncatula*. *Plant Mol. Biol.* 106, 157–172. doi:10.1007/S11103-021-01135-X
- Nakatsuka, T., Sato, K., Takahashi, H., Yamamura, S., and Nishihara, M. (2008). Cloning and characterization of the *UDP-glucose anthocyanin 5-O-glucosyltransferase* gene from blue-flowered gentian. *J. Exp. Bot.* 59, 1241–1252. doi:10.1093/jxb/ern031
- Ramsay, N. A., and Glover, B. J. (2005). MYB–bHLH–WD40 protein complex and the evolution of cellular diversity. *Trends Plant Sci.* 10, 63–70. doi:10.1016/j.tplants.2004.12.011
- Ren, Y., Zhang, N., Li, R., Ma, X., and Zhang, L. (2021). Comparative transcriptome and flavonoids components analysis reveal the structural genes responsible for the yellow seed coat color of *Brassica rapa* L. *PeerJ* 9, e10770. doi:10.7717/peerj.10770
- Selvey, S., Thompson, E. W., Matthaai, K., Lea, R. A., Irving, M. G., and Griffiths, L. R. (2001). *Beta-actin*—an unsuitable internal control for RT-PCR. *Mol. Cell. Probes* 15, 307–311. doi:10.1006/mcpr.2001.0376
- Shen, Y. H., Yang, F. Y., Lu, B. G., Zhao, W. W., Jiang, T., Feng, L., et al. (2019). Exploring the differential mechanisms of carotenoid biosynthesis in the yellow peel and red flesh of papaya. *BMC Genomics* 20, 49–11. doi:10.1186/s12864-018-5388-0
- Silan, D., He, H., Jianxin, F., and Yan, H. (2013). Advances in molecular breeding of ornamental plants. *Chin. Bull. Bot.* 48, 589–607. doi:10.3724/sp.j.1259.2013.00589
- Stanstrup, J., Broeckling, C. D., Helmus, R., Hoffmann, N., Mathé, E., Naake, T., et al. (2019). The metaRbomics toolbox in bioconductor and beyond. *Metabolites* 9, E200. doi:10.3390/metabo9100200
- Stavenga, D. G., Leertouwer, H. L., Dudek, B., and van der Kooij, C. J. (2021). Coloration of flowers by flavonoids and consequences of pH dependent absorption. *Front. Plant Sci.* 11, 2148. doi:10.3389/fpls.2020.600124
- Sterling, C. H., Veksler-Lubinsky, I., and Ambros, V. (2015). An efficient and sensitive method for preparing cDNA libraries from scarce biological samples. *Nucleic Acids Res.* 43, e1. doi:10.1093/nar/gku637
- Takeda, K., Yamashita, T., Takahashi, A., and Timberlake, C. F. (1990). Stable blue complexes of anthocyanin-aluminium-3-p-coumaroyl- or 3-caffeoyl-quinic acid involved in the blueing of *Hydrangea* flower. *Phytochemistry* 29, 1089–1091. doi:10.1016/0031-9422(90)85409-9
- Tanaka, Y., Sasaki, N., and Ohmiya, A. (2008). Biosynthesis of plant pigments: Anthocyanins, betalains and carotenoids. *Plant J.* 54, 733–749. doi:10.1111/j.1365-3113.2008.03447.X
- Tang, J., Liang, G., Dong, S., Shan, S., Zhao, M., and Guo, X. (2022). Selection and validation of reference genes for quantitative real-time PCR normalization in *Aethes dissimilis* (Lepidoptera: Noctuidae) under different conditions. *Front. Physiol.* 13, 842195. doi:10.3389/fphys.2022.842195
- Varshney, R. K., Bohra, A., Yu, J., Graner, A., Zhang, Q., and Sorrells, M. E. (2021). Designing future crops: Genomics-assisted breeding comes of age. *Trends Plant Sci.* 26, 631–649. doi:10.1016/j.tplants.2021.03.010
- Varshney, R. K., Sinha, P., Singh, V. K., Kumar, A., Zhang, Q., and Bennetzen, J. L. (2020). 5Gs for crop genetic improvement. *Curr. Opin. Plant Biol.* 56, 190–196. doi:10.1016/j.pbi.2019.12.004
- Wang, L. S., Shiraiishi, A., Hashimoto, F., Aoki, N., Shimizu, K., and Sakata, Y. (2001). Analysis of petal anthocyanins to investigate flower coloration of Zhongyuan (Chinese) and Daikon Island (Japanese) tree peony cultivars. *J. Plant Res.* 114, 33–43. doi:10.1007/PL00013966
- Xia, Z. W. B. F. (2003). Recent studies of camellia of kunming institute of botany. *China Flowers Hortic.* 10, 013.
- Xin, T., de Rieck, J., Guo, H., Jarvis, D., Ma, L., and Long, C. (2015). Impact of traditional culture on *Camellia reticulata* in Yunnan, China. *J. Ethnobiol. Ethnomed.* 11, 74. doi:10.1186/s13002-015-0059-6
- Xue, L., Wang, Z., Zhang, W., Li, Y., Wang, J., and Lei, J. (2016). Flower pigment inheritance and anthocyanin characterization of hybrids from pink-flowered and white-flowered strawberry. *Sci. Hortic. Amst.* 200, 143–150. doi:10.1016/J.SCIENTA.2016.01.020
- Yabuya, T., Yamaguchi, M. A., Imayama, T., Katoh, K., and Ino, I. (2002). Anthocyanin 5-O-glucosyltransferase in flowers of *Iris ensata*. *Plant Sci.* 162, 779–784. doi:10.1016/S0168-9452(02)00021-3
- Yamazaki, M., Gong, Z., Fukuchi-Mizutani, M., Fukui, Y., Tanaka, Y., Kusumi, T., et al. (1999). Molecular cloning and biochemical characterization of a novel anthocyanin 5-O-glucosyltransferase by mRNA differential display for plant forms regarding anthocyanin. *J. Biol. Chem.* 274, 7405–7411. doi:10.1074/JBC.274.11.7405
- Yan, H., and Kerr, W. L. (2013). Total phenolics content, anthocyanins, and dietary fiber content of apple pomace powders produced by vacuum-belt drying. *J. Sci. Food Agric.* 93, 1499–1504. doi:10.1002/JFSA.5925
- Yu, J. (1985). A Historical review and future development of *Camellia reticulata* in Yunnan. *Acta Hortic. Sin.* 2, 011.
- Yu, X., Xiao, J., Chen, S., Yu, Y., Ma, J., Lin, Y., et al. (2020). Metabolite signatures of diverse *Camellia sinensis* tea populations. *Nat. Commun.* 11, 5586–5614. doi:10.1038/s41467-020-19441-1
- Zhang, Q., Luo, J., Ma, J. L., Wei, X. J., Peng, H., Yang, S. X., et al. (2019). The complete chloroplast genome sequence of *Camellia mingii* (Theaceae), a critically endangered yellow camellia species endemic to China. *Mitochondrial DNA Part B* 4, 1338–1340. doi:10.1080/23802359.2019.1596765
- Zhao, D., and Tao, J. (2015). Recent advances on the development and regulation of flower color in ornamental plants. *Front. Plant Sci.* 6, 261. doi:10.3389/fpls.2015.00261
- Zhao, L., Gao, L., Wang, H., Chen, X., Wang, Y., Yang, H., et al. (2012). The R2R3-MYB, bHLH, WD40, and related transcription factors in flavonoid biosynthesis. *Funct. Integr. Genomics* 131 (13), 75–98. doi:10.1007/S10142-012-0301-4
- Zhao, Y., Dong, W., Wang, K., Zhang, B., Allan, A. C., Lin-Wang, K., et al. (2017). Differential sensitivity of fruit pigmentation to ultraviolet light between two peach cultivars. *Front. Plant Sci.* 8, 1552. doi:10.3389/fpls.2017.01552
- Zheng, Y., Jiao, C., Sun, H., Rosli, H. G., Pombo, M. A., Zhang, P., et al. (2016). iTAK: A program for genome-wide prediction and classification of plant transcription factors, transcriptional regulators, and protein kinases. *Mol. Plant*, 9. Shanghai Editorial Office: XLSX, 1667–1670. doi:10.1016/J.MOLP.2016.09.014/ATTACHMENT/3C4541CD-FD84-4733-A4CA-ED817E3AB26B/MMC2
- Zhou, D., Shen, Y., Zhou, P., Fatima, M., Lin, J., Yue, J., et al. (2019). Papaya *CpbHLH1/2* regulate carotenoid biosynthesis-related genes during papaya fruit ripening. *Hortic. Res.* 6, 80–13. doi:10.1038/s41438-019-0162-2
- Zhou, X., Li, J., Zhu, Y., Ni, S., Chen, J., Feng, X., et al. (2017). De novo assembly of the *Camellia nitidissima* transcriptome reveals key genes of flower pigment biosynthesis. *Front. Plant Sci.* 8, 1545. doi:10.3389/FPLS.2017.01545
- Zhu, H. H., Yang, J. X., Xiao, C. H., Mao, T. Y., Zhang, J., and Zhang, H. Y. (2019). Differences in flavonoid pathway metabolites and transcripts affect yellow petal colouration in the aquatic plant *Nelumbo nucifera*. *BMC Plant Biol.* 19, 277–318. doi:10.1186/s12870-019-1886-8